Selective tyrosine kinase inhibition by imatinib mesylate for the treatment of autoimmune arthritis

Ricardo T. Paniagua,[1,2] Orr Sharpe,[1,2] Peggy P. Ho,[3] Steven M. Chan,[1] Anna Chang,[1,2] John P. Higgins,[4] Beren H. Tomooka,[1,2] Fiona M. Thomas,[1,2] Jason J. Song,[1,2] Stuart B. Goodman,[5] David M. Lee,[6] Mark C. Genovese,[1] Paul J. Utz,[1] Lawrence Steinman,[3] and William H. Robinson[1,2]

[1]Division of Immunology and Rheumatology, Department of Medicine, Stanford University School of Medicine, Stanford, California, USA. [2]Geriatric Research, Education, and Clinical Center, Palo Alto VA Health Care System, Palo Alto, California, USA. [3]Department of Neurology and Neurological Sciences, [4]Department of Pathology, and [5]Department of Orthopedics, Stanford University School of Medicine, Stanford, California, USA. [6]Department of Medicine and Division of Rheumatology, Immunology and Allergy, Brigham and Women's Hospital, Harvard Medical School, Boston, Massachusetts, USA.

Tyrosine kinases play a central role in the activation of signal transduction pathways and cellular responses that mediate the pathogenesis of rheumatoid arthritis. Imatinib mesylate (imatinib) is a tyrosine kinase inhibitor developed to treat Bcr/Abl-expressing leukemias and subsequently found to treat c-Kit–expressing gastrointestinal stromal tumors. We demonstrate that imatinib potently prevents and treats murine collagen-induced arthritis (CIA). We further show that micromolar concentrations of imatinib abrogate multiple signal transduction pathways implicated in RA pathogenesis, including mast cell c-Kit signaling and TNF-α release, macrophage c-Fms activation and cytokine production, and fibroblast PDGFR signaling and proliferation. In our studies, imatinib attenuated PDGFR signaling in fibroblast-like synoviocytes (FLSs) and TNF-α production in synovial fluid mononuclear cells (SFMCs) derived from human RA patients. Imatinib-mediated inhibition of a spectrum of signal transduction pathways and the downstream pathogenic cellular responses may provide a powerful approach to treat RA and other inflammatory diseases.

Introduction

RA is an autoimmune synovitis affecting 0.5%–1% of the world population (1). RA is characterized by the accumulation and proliferation of inflammatory cells in the synovial (joint) lining, resulting in the formation of pannus tissue, which invades and destroys adjacent cartilage and bone. Although the etiology of RA remains unknown, macrophages, B cells, mast cells, and fibroblast-like synoviocytes (FLSs) become activated in and contribute to synovial inflammation and joint destruction. In this article we explore protein tyrosine kinase inhibition with imatinib mesylate (Gleevec, formerly STI-571) as a strategy to specifically mitigate the pathogenic responses of macrophages, B cells, mast cells, and FLSs in autoimmune arthritis and RA.

Imatinib is a small-molecule protein tyrosine kinase inhibitor developed to target the gene product of the Philadelphia chromosome *Bcr/Abl* translocation in chronic myelogenous leukemia (CML). Imatinib was initially approved by the US and European regulatory agencies for the treatment of Bcr/Abl-positive CML (2, 3) and more recently approved to treat c-Kit–expressing gastrointestinal stromal tumors (GISTs) based on its ability to antagonize c-Kit (2, 3). Along with inhibiting Abl tyrosine kinases at submicromolar concentrations, imatinib specifically and potently inhibits a narrow spectrum of tyrosine kinases including c-Fms (IC_{50} = 1.4 μM), c-Kit (IC_{50} = 0.1 μM), and PDGFRα/β (IC_{50} = 0.1 μM) (4–6).

In RA, macrophages infiltrate the synovium and secrete TNF-α and other proinflammatory cytokines that potentiate inflammation (7, 8). TNF-α plays a central role in synovitis and joint destruction in murine arthritis (9) and human RA (10), and 3 biological agents that inhibit TNF-α are approved by the US Food and Drug Administration for the treatment of RA. c-Fms is a receptor tyrosine kinase expressed on cells of the macrophage lineage and mediates growth and differentiation (11). In human peripheral blood macrophages and monocytes, imatinib inhibited LPS-induced production of TNF-α through a yet-to-be-defined c-Fms–independent mechanism (5, 12).

Mast cell activation results in release of mediators that contribute to the inflammatory and degradative processes in RA, including histamine, heparin, neutral proteases, and TNF-α (13–16). The mast cell population expands to constitute up to 5% of all synovial cells in RA (17), and mast cells and their released granule products are present in synovium and at sites of cartilage erosion in rheumatoid tissue (18, 19). c-Kit is a receptor tyrosine kinase critical for mast cell development and activation (13, 15). Mice that are mast cell deficient due to defective c-Kit signaling are resistant to induction of arthritis by transfer of K/BxN serum that contains anti–glucose-6-isomerase antibodies (20) and exhibit less severe cartilage erosion in antigen-induced arthritis (21).

Fibroblasts express PDGFR and proliferate in response to a variety of PDGF ligands. Both PDGFR and its ligands are overexpressed in RA synovial tissue, and PDGF is a potent stimulant of synovial hyperplasia in RA (22–24). A recent study suggests that imatinib inhibits PDGF-AA–induced expression of IL-1β and IL-8 as well as inhibiting downstream activation of NF-κB in rheumatoid FLSs (22).

Evidence that B cells play an important role in the pathogenesis of RA comes from human trials demonstrating the efficacy of B cell depletion with rituximab (25). It has also recently been
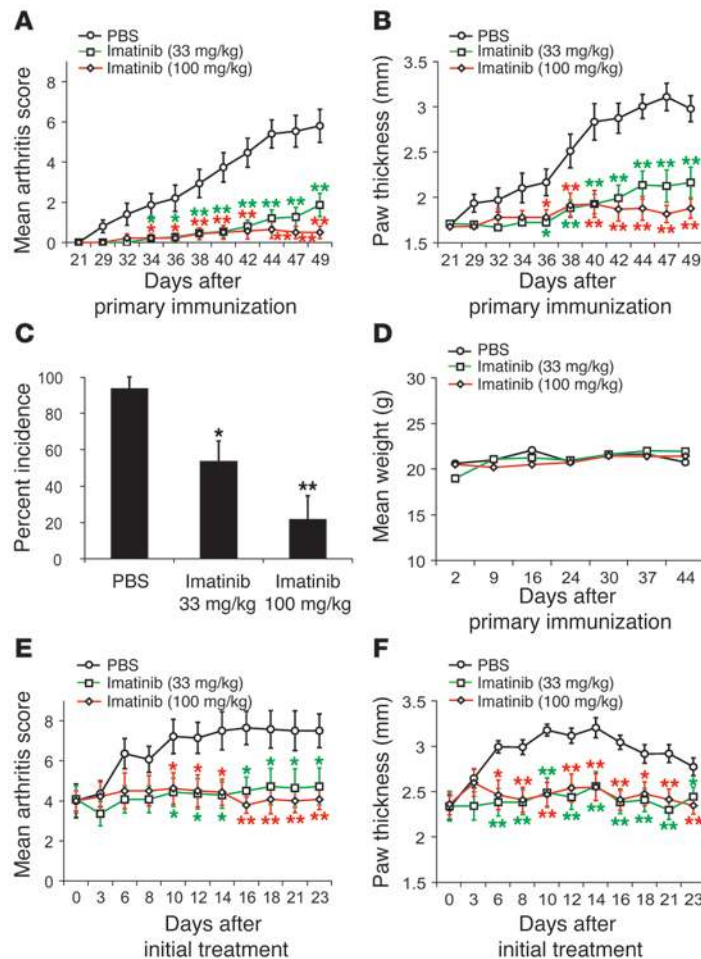
Figure 1
Imatinib prevents and treats CIA. (**A**–**D**) Prevention. DBA/1 mice were administered PBS (*n* = 15), 33 mg/kg imatinib (*n* = 15), or 100 mg/kg imatinib (*n* = 14) orally twice daily starting 1 day prior to induction of CIA. Severity of arthritis was assessed using a visual arthritis scoring system (**A**) and caliper measurements of paw thickness (**B**). The incidence of arthritis at the termination of the experiment (day 49) (**C**) and the mean weights of mice in each group (**D**) are presented. The data shown in **A** and **B** are from a representative of 3 independent experiments, each involving 14–15 mice per experimental arm. (**E** and **F**) Treatment. Following the development of clinical arthritis (average visual arthritis score of 4), DBA/1 mice with CIA were randomized and treated with PBS (*n* = 14), 33 mg/kg imatinib (*n* = 14), or 100 mg/kg imatinib (*n* = 14) orally twice daily, and disease was monitored using a visual arthritis scoring system (**E**) and paw thickness measurements (**F**). Values from the presented results are the mean ± SEM for this representative experiment. *$P < 0.05$, **$P < 0.01$ compared with PBS-treated mice.

demonstrated that anti–cyclic citrullinated peptide (anti-CCP) antibodies can predate the clinical diagnosis of RA by years (26) and that anti-citrulline antibodies can exacerbate experimental arthritis in mice (27).

Recent case reports describe 2 patients, one with RA and CML and the other with RA and GIST, who when treated with imatinib experienced improvement in the clinical features of RA (28, 29). In an evaluation of imatinib in 3 patients with severe RA, 1 patient did not exhibit a meaningful response, while 2 patients exhibited trends toward improvement (29). Whether

the tyrosine kinase inhibitor imatinib can provide benefit in mouse models of autoimmune arthritis has not been previously determined.

Based on the ability of imatinib to inhibit mast cell c-Kit, FLS PDGFR, and macrophage c-Fms as well as the above-described case reports, we investigated the efficacy and mechanisms of imatinib in the collagen-induced arthritis (CIA) model of RA. We extended our studies to SFMCs and FLSs derived from human RA patients. We demonstrate that imatinib prevents and treats established CIA. We further demonstrate that imatinib selectively inhibits a diverse set of signal transduction pathways that initiate cellular responses in macrophages, B cells, mast cells, and fibroblasts that mediate synovitis, pannus formation, and joint destruction in RA.

Results

Imatinib reduces the incidence and severity of CIA. We performed experiments to determine the ability of imatinib to prevent and treat autoimmune arthritis in the CIA model. CIA was induced by injecting DBA/1 mice with bovine type II collagen (CII) emulsified in CFA, followed by boosting 21 days later with CII emulsified in incomplete Freund's adjuvant (IFA). Mice were dosed orally twice daily with 100 mg/kg or 33 mg/kg imatinib based on the published pharmacokinetic profiles of imatinib metabolism in mice and humans (2, 4, 30). Imatinib is metabolized more rapidly in mice than in humans, and mice receiving a twice-daily oral dose of 100 mg/kg imatinib exhibit a pharmacokinetic profile similar to that in humans on a mid-range dose of 400 mg once daily. This dosing regimen for mice and humans results in mean peak and trough plasma levels of 4.6–6 μM and 1–1.5 μM, respectively (2, 30).

For the CIA prevention studies, oral administration of imatinib was initiated 1 day prior to induction of CIA. Mice treated with either 33 or 100 mg/kg imatinib displayed significant reductions in the severity of CIA based on reduced paw swelling, erythema, and joint rigidity as assessed by the mean visual arthritis score (Figure 1A) and reduced mean paw thickness (Figure 1B) ($P < 0.01$ by Mann-Whitney *U* test for both the 33 and 100 mg/kg groups after day 38 following primary immunization). Imatinib also reduced the incidence of CIA (Figure 1C). The therapeutic effects of imatinib demonstrated a trend toward dose dependence (Figure 1, A–C). These results are representative of 3 independent experiments. There was no apparent toxicity or weight loss (Figure 1D) in mice receiving imatinib.

For the CIA treatment studies, mice with established clinical arthritis (average visual score of 4) were randomized and treated with 33 or 100 mg/kg imatinib or PBS. Both the 33 and 100 mg/kg dose levels of imatinib inhibited the progression of established arthritis as assessed by both the visual scoring system (Figure 1E) and mean paw thickness (Figure 1F) ($P < 0.05$ or $P < 0.01$ after 10 days following the initiation of treatment).

Histopathologic analysis was performed on hind paws harvested from mice with CIA receiving imatinib or PBS in the prevention and treatment experiments. Representative images of H&E-stained joint tissue sections from imatinib- and PBS-treated mice in the CIA prevention studies are presented (Figure 2A). Histopathologic evaluation by an investigator blinded to treatment group demonstrated that imatinib resulted in statistically significant reductions in synovitis, pannus, and erosion scores in both the CIA prevention (Figure 2B;
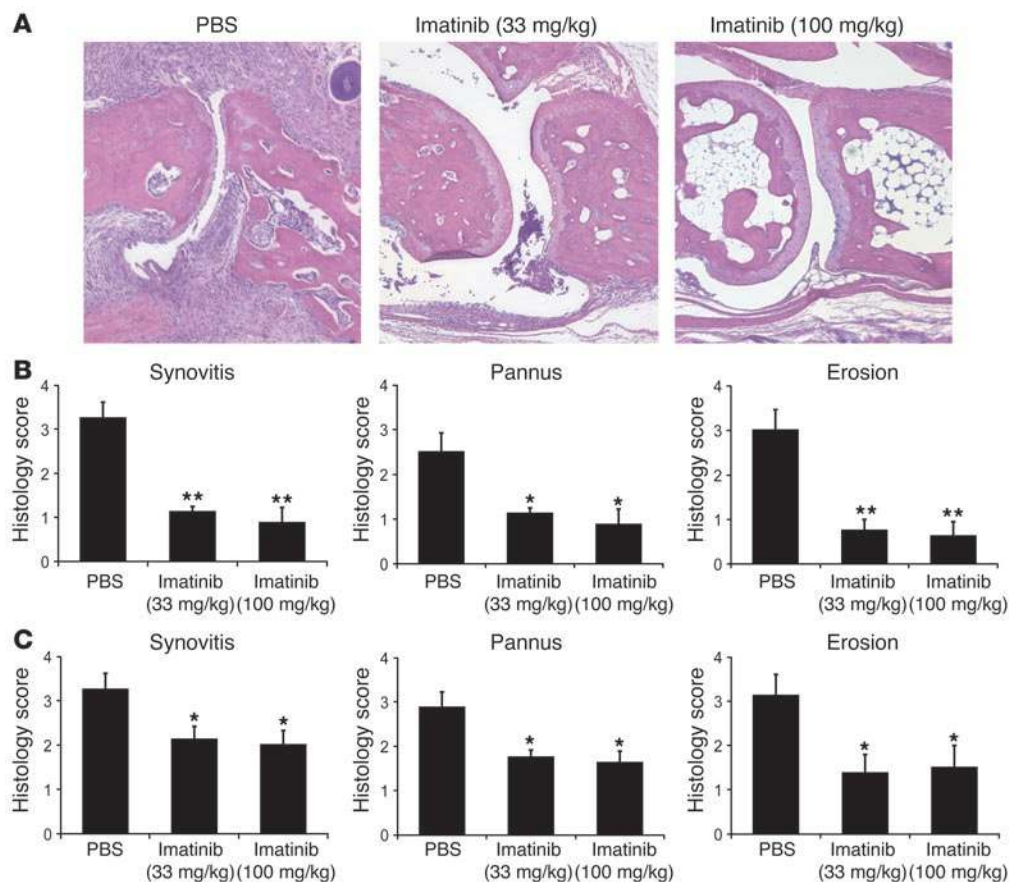
Figure 2
Imatinib reduces synovitis, pannus formation, and joint erosions in CIA. (**A**) Representative H&E-stained joint tissue sections from DBA/1 mice from a CIA prevention study. (**B** and **C**) Histopathological scores of inflammation, pannus formation, and bone and cartilage erosions in DBA/1 mice with CIA in the prevention (**B**; PBS, $n = 8$; 33 mg/kg imatinib, $n = 8$; 100 mg/kg imatinib, $n = 8$) and treatment (**C**; PBS, $n = 8$; 33 mg/kg imatinib, $n = 8$; 100 mg/kg imatinib, $n = 8$) studies. Values are mean ± SEM. *$P < 0.05$, **$P < 0.01$ compared with PBS-treated group.

$P < 0.01$ by Mann-Whitney U test for synovitis and erosion scores; $P < 0.05$ for pannus scores) and established CIA treatment (Figure 2C; $P < 0.05$ for synovitis, pannus, and erosions scores) experiments. Thus, imatinib was effective at both preventing and treating established CIA based on clinical and histopathologic analyses.

Imatinib inhibits mast cell production of proinflammatory cytokines. Based on the observation that significant numbers of mast cells are present in synovial tissue derived from human RA patients (18, 19), we characterized the effects of imatinib on activation of the cloned murine mast cell line C1.MC/57.1 (31). C1.MC/57.1 mast cells expand in a growth factor–independent fashion, and although growth does not depend on SCF, C1.MC/57.1 mast cells respond to SCF by secreting cytokines (32, 33). C1.MC/57.1 mast cells were stimulated with 100 ng/ml SCF for 48 hours in the presence of 0–5 μM imatinib, and cytokine analysis was performed on culture supernatants using a bead-based cytokine assay. Imatinib at 1 and 5 μM dramatically reduced mast cell production of TNF-α, GM-CSF, and IL-6 to levels similar to those in the unstimulated cell populations (Figure 3A).

Imatinib inhibits mast cell signaling by SCF. To comprehensively characterize tyrosine kinase activation states and signal transduction pathways modulated by imatinib, IB and reverse phase protein (RPP) lysate array (34) analyses were performed. Mast cells were pretreated with 0–5 μM imatinib and stimulated with SCF for 10 minutes. Lysates were generated for IB and RPP lysate arrays. IB demonstrated that imatinib potently inhibited SCF-induced phosphorylation of c-Kit (Figure 3B), with a corresponding reduction in phosphorylation of downstream Akt (Ser473) (Figure 3C). RPP arrays were generated by printing cellular lysates on nitrocellulose-

coated microscope slides, followed by incubation with phospho-specific antibodies and fluorescence-based detection of antibody binding to ascertain the activation of protein tyrosine kinases in the MAPK family and other pathways.

RPP array analysis revealed that 1 and 5 μM imatinib inhibited SCF-induced activation of diverse protein tyrosine kinases downstream of c-Kit, including members of MAPK pathways including ERK, JNK, and p38 (Figure 3D). Imatinib also prevented phosphorylation of the signaling molecules Akt (Ser473 and Thr308), p70S6K, and Raf (Figure 3D). Imatinib-mediated inhibition of c-Kit and Akt phosphorylation (Ser473) was also observed in IB analysis (Figure 3C), which served as validation for RPP array results. Together, the IB and RPP array data demonstrate that imatinib potently inhibits SCF-induced activation of MAPK and other pathways that mediate mast cell activation and proinflammatory cytokine production.

Mast cells are present in inflamed CIA synovial tissue. To confirm prior observations that mast cells are present in joints derived from mice with CIA (35), sections of CIA joints were stained with toluidine blue. Toluidine blue is a metachromatic dye that stains the strongly sulphated acid mucopolysaccharide (heparin) content of mast cell granules. Toluidine blue staining revealed significant numbers of mast cells in inflamed CIA synovial tissue (Figure 3E).

Imatinib inhibits macrophage signal transduction events. M-CSF is present in RA synovial tissue and has been shown to exacerbate CIA (36). To determine whether imatinib affects M-CSF–mediated signal transduction in macrophages, IB and RPP arrays were applied to characterize lysates generated from resident peritoneal
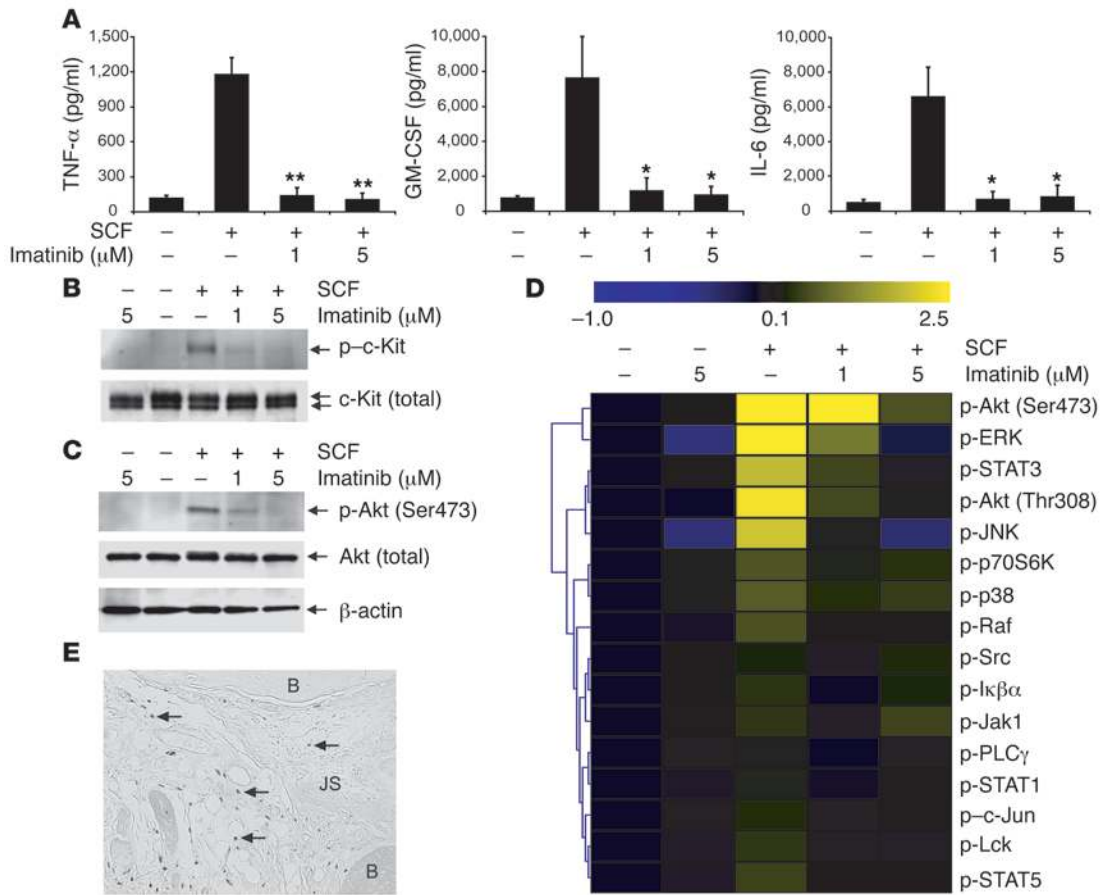
Figure 3
Imatinib inhibits mast cell c-Kit activation and proinflammatory cytokine production. (**A**) C1.MC/57.1 mast cells were stimulated with 100 ng/ml SCF in the presence of 0–5 μM imatinib, and after 48 hours culture supernatants were collected and analyzed for TNF-α, GM-CSF, and IL-6 by a bead-based cytokine assay. Values are mean ± SEM. *$P < 0.05$, **$P < 0.01$ compared with stimulated cells without imatinib. (**B** and **C**) C1.MC/57.1 mast cells were serum starved, preincubated with imatinib, and stimulated with 100 ng/ml SCF for 10 minutes in the presence or absence of imatinib, and lysates were generated for IB analysis. IBs were probed with antibodies specific for phospho–c-Kit and total c-Kit (**B**) and phospho-Akt (Ser473) and total Akt (**C**). (**D**) Mast cell lysates generated using the stimulation conditions described in **B** and **C** were printed to generate RPP arrays. RPP arrays were probed with a variety of antibodies specific for phosphorylated (activated) protein tyrosine kinases and levels normalized to levels in unstimulated cells. Yellow represents anti-protein tyrosine kinase antibody reactivity, and blue represents lack of reactivity. (**E**) Mast cells are present in CIA synovium. A representative joint section from a mouse with CIA was stained with toluidine blue. Mast cells present in the densely inflamed CIA synovial tissue are indicated by arrows. B, bone; JS, joint space. Original magnification, ×200.

macrophages. Resident peritoneal macrophages were isolated from DBA/1 mice, pretreated with imatinib, and stimulated with 100 ng/ml M-CSF for 10 minutes and lysates generated for analysis. IB demonstrated that 1 and 5 μM imatinib inhibited M-CSF–induced phosphorylation of c-Fms, while levels of total c-Fms were similar in all samples (Figure 4A). The downstream signaling molecule Akt (Ser473) also exhibited reduced phosphorylation in imatinib-pretreated macrophages (Figure 4B).

RPP array analysis of M-CSF–stimulated macrophage lysates demonstrated that imatinib blocked phosphorylation of protein tyrosine kinases in the MAPK family and other pathways downstream of c-Fms, including Akt (Ser473 and Thr308), ERK, JNK, and p38 (Figure 4C). Thus, the IB and RPP array data demonstrate that imatinib potently inhibits M-CSF–induced macrophage activation through c-Fms.

Imatinib inhibits B cell proliferation and immunoglobulin production in vitro. B cells from naive DBA/1 mice were isolated from whole sple-

nocytes, and their purity was verified by flow cytometry (data not shown). Isolated B cells were stimulated for 72 hours with anti-IgM (50 μg/ml) or LPS (5 μg/ml) in the presence or absence of 1–10 μM imatinib. B cell proliferation induced by anti-IgM was inhibited by imatinib concentrations as low as 5 μM ($P < 0.001$; Figure 5A). Imatinib inhibited LPS-stimulated B cell proliferation in a dose-dependent fashion ($P < 0.001$ for concentrations of 1 μM and higher) (Figure 5A). Further, IgM production by LPS-stimulated B cells was mildly reduced by imatinib at a concentration of 1 μM, and the most significant reduction occurred at 10 μM (Figure 5B).

Imatinib reduces epitope spreading of autoreactive B cell responses in CIA. Synovial antigen microarrays were generated that contained proteins and peptides representing a spectrum of candidate autoantigens in RA and CIA (37, 38). Synovial arrays were probed with sera derived from mice in CIA prevention studies that were dosed with 100 mg/kg imatinib or PBS, followed by Cy3-labeled secondary antibody to detect bound antibodies. Figure 5C presents the
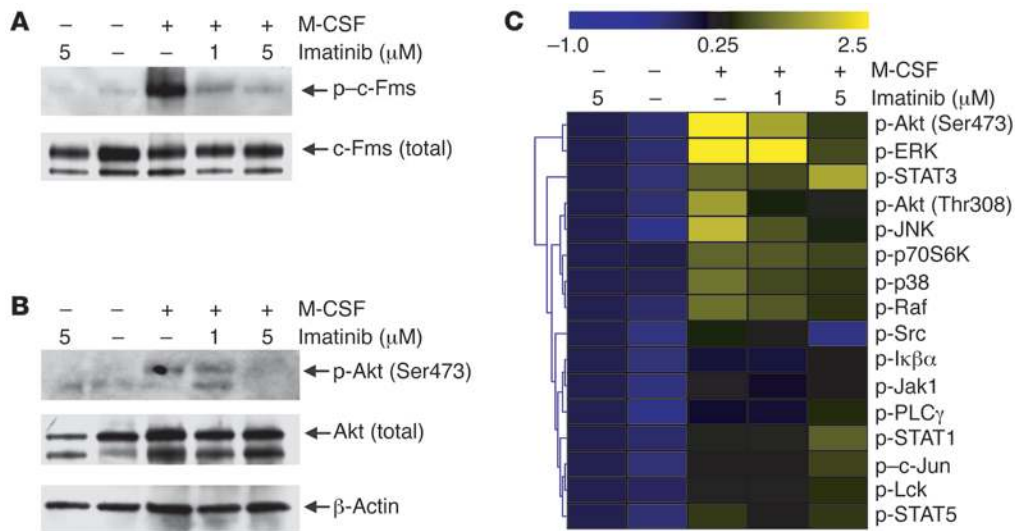
Figure 4
Inhibition of macrophage c-Fms and downstream MAPK pathways by imatinib. (**A** and **B**) Isolated resident peritoneal macrophages were serum starved, preincubated with imatinib, and stimulated with 100 ng/ml M-CSF for 10 minutes in the presence of imatinib and lysates generated for IB analysis. IBs were probed with antibodies specific for phospho–c-Fms and total Fms (**A**) or phospho–Akt (Ser473) and total Akt (**B**). (**C**) Peritoneal macrophage lysates generated using the stimulation conditions described in **A** and **B** were printed on RPP arrays. RPP arrays were probed with a variety of antibodies specific for MAPK pathway and other protein tyrosine kinases, and normalized kinase levels displayed as a heatmap.

protein and peptide antigens (out of more than 500 total proteins and peptides contained on synovial arrays) identified by the significance analysis of microarrays (SAM; ref. 39) algorithm as exhibiting statistically increased autoantibody reactivity in sera derived from PBS- as compared with imatinib-treated mice (false discovery rate [FDR], <0.06). A hierarchical cluster algorithm was applied to organize mice and SAM-identified antigen features based on the degree of similarity of their autoantibody reactivity profiles, and the results presented as a heatmap. The heatmap of autoantibody reactivity demonstrates that PBS-treated mice with CIA (the results for these mice cluster together on the left side of the heatmap image) exhibited expansion of their autoantibody responses to target multiple candidate autoantigens (intermolecular epitope spreading). Further, the heatmap demonstrates that in vivo treatment of CIA mice with imatinib (results for these mice cluster together on the right side of the heatmap image) reduced expansion of autoreactive B cell responses to native epitopes representing glycoprotein 39 (gp39), clusterin, histone 2B (H2B), and hnRNPB1 as well as to citrullinated epitopes derived from filaggrin (cyc-filaggrin, cfc8, and CCP cyc Ala-12) and clusterin (Figure 5C).

Anti-collagen T cell proliferation and cytokine production are inhibited by imatinib. We further investigated the impact of imatinib on T cells expressing a transgenic TCR specific for CII peptide 257-72 (40). When stimulated in the presence of 1 or 3.3 μM imatinib, CII-specific T cells proliferated robustly to heat-denatured whole CII, while 10 μM imatinib (exceeding the 1–4.6 μM blood level achieved by a mid-range human dose; refs. 2, 3) potently inhibited proliferation (Figure 6A). A moderate reduction in production of proinflammatory IFN-γ by CII-stimulated TCR transgenic T cells was observed at 3.3 μM imatinib, while supratherapeutic 10 μM imatinib further reduced production of the immunomodulatory cytokines IFN-γ, TNF-α, and IL-4 (Figure 6B). Anti-CII T cell production of IL-2

in response to CII was not significantly reduced at any of the imatinib concentrations tested (Figure 6B). In these experiments, the T cells appeared viable, and 10 μM imatinib did not result in staining with annexin V (a marker for early apoptosis) or propidium iodide (a marker for cell death) as determined by flow cytometry analysis (data not shown).

Imatinib inhibits TNF-α production by human RA SFMCs. Mononuclear cells were isolated from synovial fluid derived from RA patients. Because M-CSF induces mononuclear cell maturation but not TNF-α production (11), we utilized LPS to stimulate SFMCs to produce TNF-α (5, 12), the archetypal proinflammatory cytokine in RA. SFMCs were stimulated in vitro with LPS for 48 hours in the presence of 0–8 μM imatinib. Bead-based cytokine analysis of culture supernatants demonstrated reductions in production of proinflammatory cytokines including TNF-α and to a lesser degree IL-12, but imatinib did not inhibit LPS-induced production of IL-1α (Figure 7A).

Imatinib inhibits proliferation and PDGFRβ signaling in human RA FLSs. FLSs were isolated from pannus derived from a human RA patient at the time of knee arthroplasty. For the proliferation experiments, FLSs were grown in vitro and stimulated with 25 ng/ml PDGF-BB in the presence of 0–6 μM imatinib, and proliferation was measured by [³H]thymidine incorporation. Imatinib concentrations as low as 0.25 μM inhibited PDGF-BB–induced fibroblast proliferation (Figure 7B). To determine the affects of imatinib on FLS signaling, FLSs were stimulated with PDGF-BB with or without preincubation with 0–5 μM imatinib. Imatinib at 0.5 and 5 μM potently inhibited phosphorylation of PDGFRβ (Figure 7C) as well as the downstream signaling molecule Akt (Figure 7D).

Discussion

In this study we demonstrate that imatinib robustly prevents and treats CIA by selectively inhibiting a spectrum of signal transduction pathways central to the pathogenesis of RA. We demonstrate that imatinib abrogates PDGFR signaling in human RA patient FLSs; c-Kit activation in as well as production of proinflammatory cytokines by mast cells; LPS-induced TNF-α production by SFMCs; and T and B lymphocyte function. Our in vivo and in vitro data indicate that imatinib potently inhibits diverse cellular responses that play critical roles in driving synovitis, pannus formation, and joint destruction in RA.

Mast cells influence both innate and adaptive immunity (41), are present in rheumatoid synovial tissues, and may play an important role in the pathogenesis of RA (13–15, 20). Further, mast cells in human RA synovial tissue express TNF-α (19). Using IB and
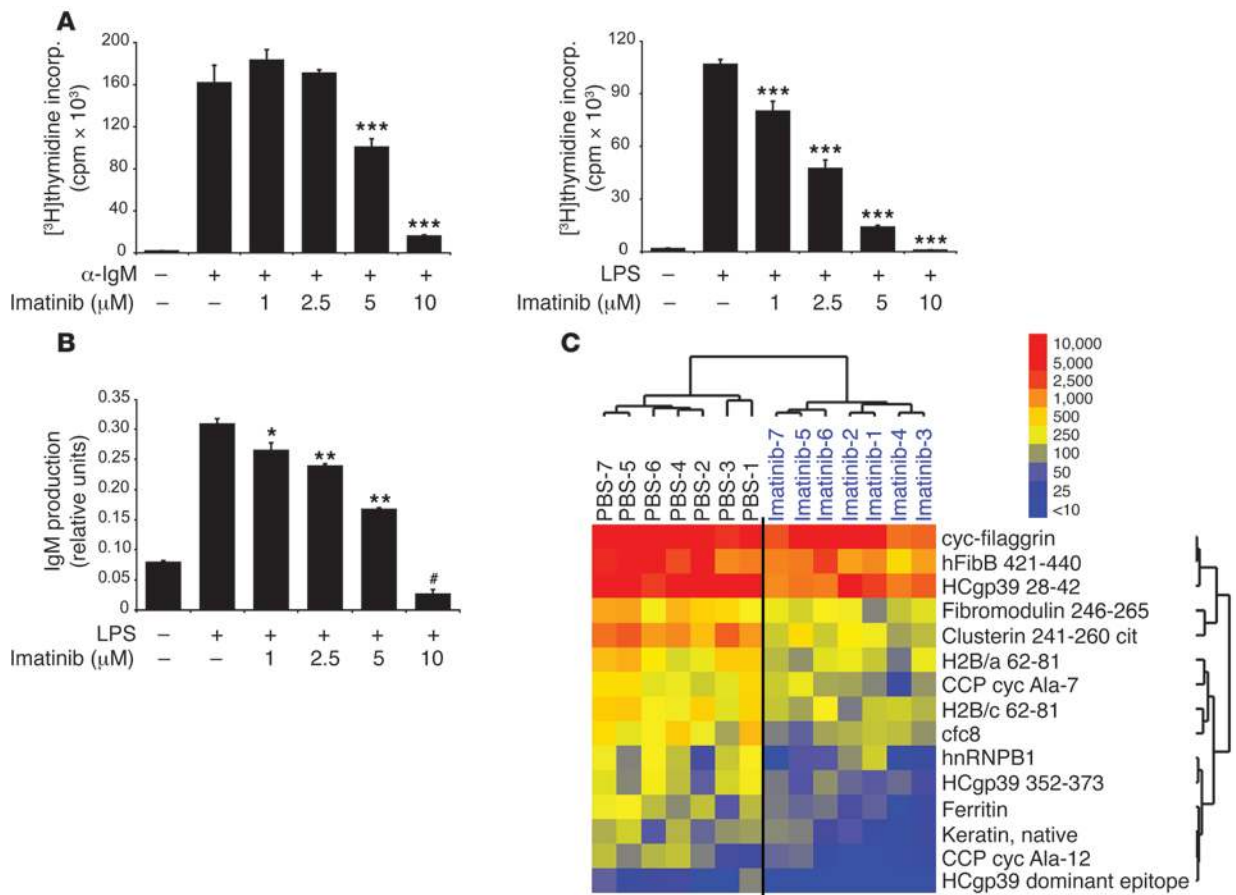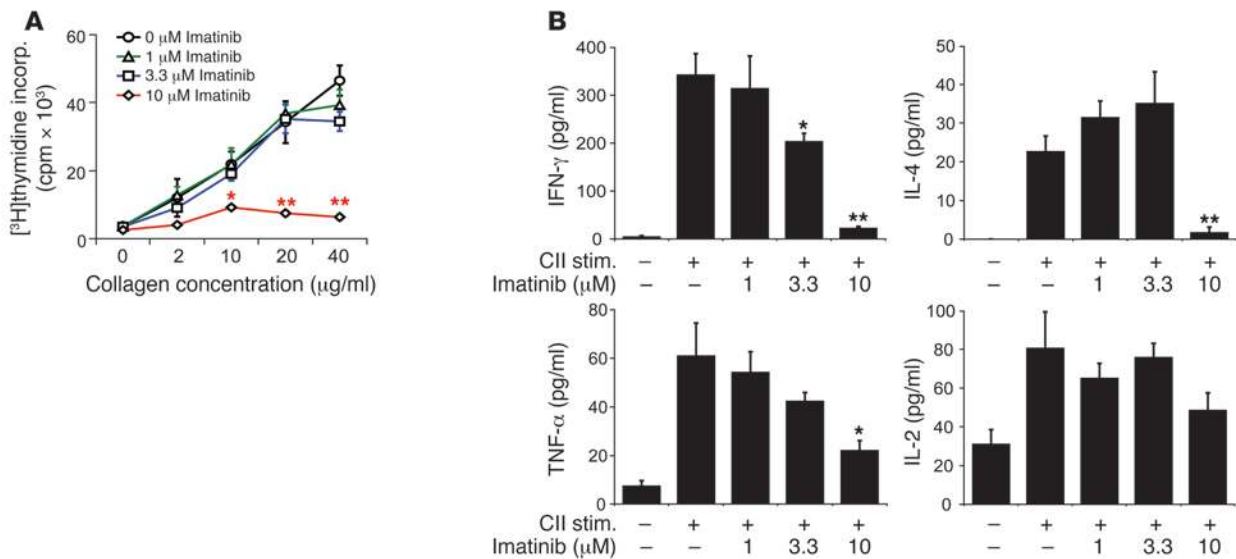
Figure 5
Imatinib inhibits B cell proliferation and Ig production in vitro and autoreactive B cell epitope spreading in vivo. (**A**) B cells from naive DBA/1 mice were stimulated with 50 μg/ml IgM or 5 μg/ml LPS in the presence of 0–10 μM imatinib. After 48 hours, B cells were pulsed with [³H]thymidine for 18 hours. Data represent mean cpm ± SEM of quadruplicates and are representative of 3 independent experiments. incorp., incorporation. (**B**) B cells stimulated with LPS (5 μg/ml) were cocultured with 0–10 μM imatinib, and IgM production was measured by ELISA. *P < 0.05, **P < 0.01, ***P < 0.001 compared with stimulated cells without imatinib. (**C**) Synovial array profiling of serum autoantibodies derived from mice with CIA treated with PBS (n = 7) or 100 mg/kg imatinib (n = 7) (day 49). Synovial microarrays containing candidate autoantigens in RA and CIA were incubated with 1:150 dilutions of mouse sera; autoantibody binding was detected with Cy3-labeled anti-mouse IgG/M secondary antibody; and arrays were scanned to quantify autoantibody binding to each antigen feature. SAM was applied to identify antigen features with statistical differences in autoantibody reactivity in samples derived from PBS-treated mice as compared with imatinib-treated mice (false discovery rate, 0.06). Cluster software was used to order results for the mice and the SAM-identified antigen features, and TreeView software was used to display the resulting clusters of autoantibody reactivity as a heatmap. Red represents positive reactivity, yellow intermediate reactivity, and blue lack of reactivity. Numbers in the key represent digital fluorescence intensity units.

RPP array technology, we demonstrated that imatinib inhibits SCF-induced c-Kit phosphorylation and downstream activation of MAPK pathways in mast cells. Further, imatinib inhibited SCF-induced mast cell production of the inflammatory cytokines TNF-α, IL-6, and GM-CSF. These data suggest that imatinib-mediated inhibition of mast cell activation could contribute to its efficacy in CIA and potentially human RA.

PDGFR and PDGF are overexpressed in RA synovial tissue (22). Our data suggest that imatinib-mediated inhibition of PDGFR signaling could reduce FLS proliferation and pannus formation and thereby provide clinical benefit in RA. It is an intriguing possibility that antagonism of fibroblast proliferation by imatinib might also provide efficacy in scleroderma, idiopathic pulmonary fibrosis (42), and other inflammatory diseases in which fibrotic processes play dominant roles in mediating pathogenesis.

c-Fms is expressed predominantly on cells of the macrophage cell lineage and stimulates macrophage proliferation, differentiation, and survival (5, 11). We demonstrated that imatinib inhibits SFMC production of TNF-α in response to LPS; however, the exact pathway involved remains to be defined (5, 12). Imatinib-mediated inhibition of monocyte/macrophage proliferation, differentiation, and TNF-α production could reduce disease activity in RA.

We demonstrated that imatinib decreased B cell proliferation in response to both anti-IgM and LPS stimulation as well as IgM production in response to LPS stimulation. In vivo treatment of mice with CIA with imatinib reduced epitope spreading of the autoantibody response (Figure 5C), and we have observed similar reductions in epitope spreading in other models of autoimmunity following effective therapy (27, 43, 44). c-Abl phosphorylates and

Figure 6
Supratherapeutic imatinib concentrations inhibit T cell responses. (**A**) Splenocytes derived from a mouse expressing a transgene encoding a CII-specific TCR were stimulated with 0–40 μg/ml heat-denatured whole CII in the presence of 0–10 μM imatinib. [³H]thymidine incorporation was used to measure proliferation of CII-specific T cells. (**B**) Bead-based cytokine analysis of culture supernatants from anti-CII TCR transgenic splenocytes stimulated with 20 μg/ml CII from **A**. Values are mean ± SEM. *$P < 0.05$, **$P < 0.01$ compared with stimulated cells without imatinib. stim., stimulation.

colocalizes with CD19 on the B cell surface following stimulation of the B cell antigen receptor (BCR), and c-Abl–deficient mice have defective BCR signaling (45). Since imatinib blocks c-Abl kinase activity at submicromolar concentrations (4, 6), it is possible that imatinib inhibits B cell proliferation and IgM production in vitro and reduces expansion of autoreactive B cell responses in CIA in vivo by inhibiting BCR signaling.

A role for autoreactive T cells in RA is supported by the presence of T cell infiltrates in rheumatoid synovium and the efficacy of CTLA4-Ig (1, 46). In vitro studies suggest that imatinib attenuates T cell activation via inhibition of the TCR-associated tyrosine kinase Lck (47). Our in vitro studies demonstrate that imatinib only inhibited anti-CII T cell proliferation at 10 μM, the highest concentration tested. It remains unclear what impact the clinically utilized dose of imatinib, from which blood levels of 1–4.6 μM are achieved (2), will have on T cell responses in vivo.

Imatinib inhibits a select set of tyrosine kinases that are directly implicated in the pathogenesis of RA, distinguishing it from general tyrosine kinase inhibitors such as genistein. Genistein was identified in the mid-1980s as a pan-tyrosine kinase inhibitor (48, 49) and has been investigated in experiments utilizing RA synovial cells (50, 51). Genistein inhibited RA synovial cell proliferation (50) and RA FLS chemokine mRNA expression in response to IL-17 stimulation (51). Verdrengh and colleagues explored the use of genistein in CIA (52). Although they observed statistically significant reductions in anti-collagen antibodies as well as trends toward reductions in synovitis, cartilage and bone destruction, arthritis incidence, and mean arthritis severity in genistein-treated mice with CIA, they concluded that "Clinically, the arthritis of collagen II exposed mice was not improved upon treatment with genistein in CIA" (52). It is likely that genistein, as a pan-tyrosine kinase inhibitor, is significantly more toxic than imatinib, thereby prohibiting the use of dosing regimens sufficient to achieve effective inhibition of the relevant kinases in CIA (52). In contrast

to genistein, imatinib is highly specific for Abl tyrosine kinases, PDGFR, c-Kit, and c-Fms at concentrations achieved in typical human dosing regimens (6, 53).

Recent data suggest that the inhibitory effect of imatinib on M-CSF– and soluble RANKL–induced osteoclast formation could also contribute to its efficacy in RA (54). Ando and colleagues observed that, after the development of clinical arthritis, rats treated with imatinib experienced a reduction in joint destruction and pannus formation (54).

In addition to potentially providing benefit in RA, it is anticipated that imatinib could also provide efficacy in other autoimmune diseases. A patient with psoriasis exhibited clinical improvement following treatment with imatinib for a concomitant malignancy (55). Imatinib ameliorated glomerulonephritis in MRL/lpr mice, and this effect was attributed to inhibition of PDGFR (56). Mast cells, which are potently inhibited by imatinib, have been suggested to contribute to pathogenesis of multiple sclerosis, autoimmune skin diseases, and inflammatory bowel disease (15). TNF-α is a driver of autoimmune tissue injury in a spectrum of autoimmune diseases, including RA, Crohn disease, psoriasis, and multiple sclerosis (57). Although imatinib-mediated inhibition of macrophage TNF-α production, mast cell activation and TNF-α release, and autoreactive B and T lymphocyte activation could provide benefit in many autoimmune diseases, imatinib's ability to inhibit PDGFR makes it particularly suited for the treatment of RA and other diseases in which fibrotic processes play a central role in pathogenesis.

In conclusion, we have shown that imatinib potently treats CIA and inhibits multiple signal transduction pathways that drive pathogenic cellular responses in RA. Our results provide further rationale for prospective clinical trials to determine whether imatinib provides efficacy in RA and other autoimmune diseases. Selective tyrosine kinase inhibition by imatinib and other pharmacologic agents (58) represents a promising and powerful strategy for the treatment of RA and other inflammatory diseases.
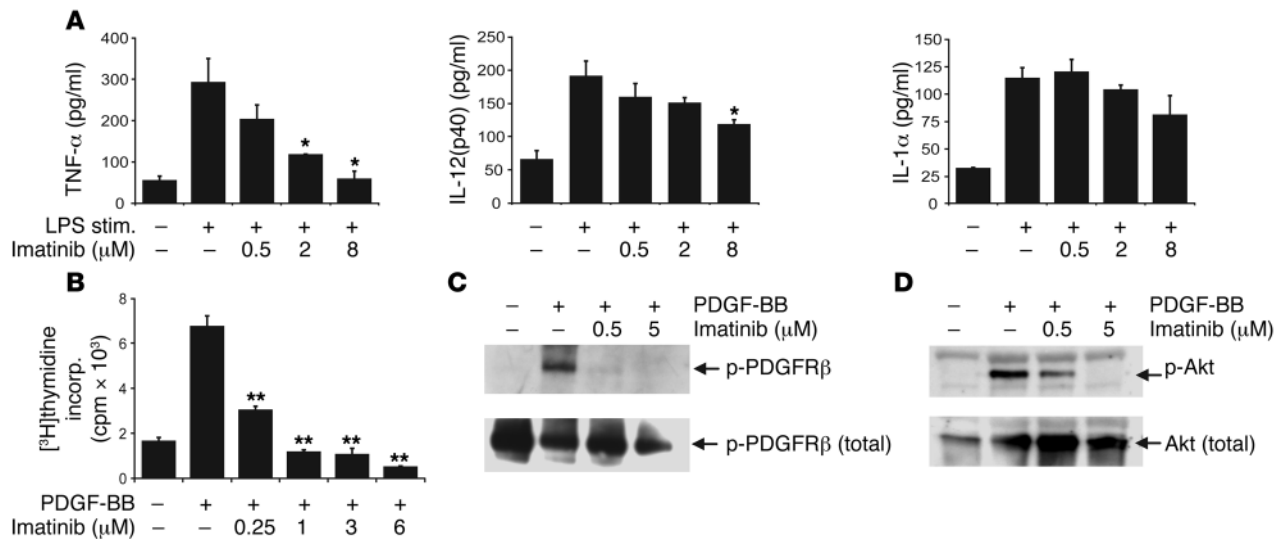
Figure 7

Imatinib inhibits SFMC cytokine production and FLS PDGFRβ signaling. (**A**) Imatinib inhibits cytokine production by SFMCs derived from a human RA patient. SFMCs were stimulated with 100 ng/ml LPS in the presence of 0–8 μM imatinib, and after 48 hours culture, supernatants were analyzed for TNF-α, IL-12(p40), and IL-1α. Values are mean ± SEM. *$P < 0.05$ compared with stimulated cells without imatinib. Results are representative of independent experiments performed on SFMCs isolated from 2 RA patients. (**B**) Modulation of FLS proliferation by imatinib. FLSs from a human RA patient were incubated with 25 ng/ml PDGF-BB in the presence of 0–6 μM imatinib. After 48 hours, FLS cultures were pulsed with [³H]thymidine for 18 hours. Data represent mean cpm ± SEM of quadruplicates and are representative of experiments involving FLS lines derived from 4 RA patients. **$P < 0.001$ compared with stimulated cells without imatinib. (**C** and **D**) Imatinib inhibits PDGFRβ activation in FLS derived from a human RA patient. Cultured FLSs were preincubated with imatinib for 3–4 hours followed by stimulation with 25 ng/ml PDGF-BB for 10 minutes. Lysates were generated and IB analysis performed with antibodies specific for phospho-PDGFRβ and total PDGFRβ (**C**) and phospho-Akt and total Akt (**D**). IBs are representative of independent experiments performed on FLS lines derived from 4 RA patients.

Methods

Cell lines, antibodies, and imatinib mesylate. The mouse mast cell line C1.MC/57.1 was provided by S. Galli (Stanford University) (31, 33). Anti-c-Fms and anti-PDGFRβ were from Santa Cruz Biotechnology Inc., and anti–β-actin was from Sigma-Aldrich; all other antibodies were from Cell Signaling Technology. Imatinib mesylate tablets (purchased from Stanford Inpatient Pharmacy Services) were ground, and imatinib was extracted by vigorous shaking overnight in acetate buffer, pH 5.0, followed by a 30-minute centrifugation to remove auxiliary particulate substances. To address the possibility that auxiliary substances used to formulate imatinib in tablets were responsible for its in vitro effects, we obtained chemically synthesized (pure) imatinib that was produced and confirmed to be more than 95% pure by the Organic Synthesis Core Facility at Memorial Sloan-Kettering Cancer Center, as described previously (59). Pure imatinib was utilized for the in vitro mast cell cytokine release (Figure 3A) and B cell proliferation (Figure 5A) assays, and no differences in the inhibitory profiles of extracted as compared with chemically synthesized imatinib were observed in in vitro assays (data not shown).

Animals. Six- to eight-week-old male DBA/1 mice (The Jackson Laboratory) were housed at Stanford University and experiments performed under protocols approved by the Stanford University Committee of Animal Research and in accordance with NIH guidelines. Mice expressing a TCR specific for CII were provided by W. Ladiges (University of Washington, Seattle, Washington, USA) (40).

Human RA synovial fluid and tissue samples. Human synovial fluid and tissue samples were collected under Stanford University Institutional Review Board–approved protocols and after provision of informed consent by patients with the diagnosis of RA (60).

CIA studies. CIA in DBA/1 mice was induced and scored as described previously (61). In brief, DBA/1 mice received intradermal immunization with 100 μg/mouse bovine CII (Chondrex) emulsified in CFA containing 250 μg/mouse heat-killed *Mycobacterium tuberculosis* H37Ra (BD). Twenty-one days following immunization, mice were boosted by subcutaneous injection at the base of the tail with 100 μg/mouse bovine CII emulsified in IFA. For the treatment experiments, only mice with clinical arthritis (average visual arthritis score of 4) were randomized and treated. Mice were scored for arthritis using the following visual scoring system: grade 0, no swelling or erythema; grade 1, mild swelling and erythema or digit inflammation; grade 2, moderate swelling and erythema confined distal to the mid-paw; grade 3, more pronounced swelling and erythema with extension to the ankle; grade 4, severe swelling, erythema, and joint rigidity of the ankle, foot, and digits. Each limb was graded with a score of 0–4, with a maximum possible score of 16 for each individual mouse. Paw thickness was determined by measuring the thickness of the most severely affected hind paw with 0- to 10-mm calipers. Imatinib was diluted in PBS, and 33 mg/kg or 100 mg/kg delivered by oral gavage twice daily, starting on the day prior to CIA induction for the prevention experiments and following development of arthritis and randomization for the treatment experiments.

Histopathology studies. Hind limbs were fixed and decalcified in Cal-Ex II (Fischer Scientific) for 3 days prior to embedding in paraffin. Sections were stained with H&E and evaluated by an investigator blinded to treatment status for synovitis, pannus formation, and bone and/or cartilage destruction based on a previously described scoring system: grade 0, normal; grade 1, mild inflammation, mild hyperplasia of the synovial lining layer, mild cartilage destruction without bone erosion; grades 2–4, increasing degrees of inflammatory cell infiltrates, synovial lining hyperplasia, and pannus formation and cartilage and bone destruction (62).

Isolation and stimulation of RA synovial cells. RA SFMCs were isolated using a Ficoll-Hypaque density gradient (Amersham Biosciences) and selected by adherence to plastic. Isolated SFMCs were stimulated with LPS (100 ng/ml; Sigma-Aldrich) for 48 hours. Unstimulated SFMCs treated or untreated with imatinib exhibited greater than 75% viability based on trypan blue staining, and viability was similar in the imatinib- and control-treated cultures (data not shown). RA FLSs were isolated from remnant pannus obtained at knee arthroplasty. Pannus was minced; digested at 37°C for 75 minutes with 1 mg/ml collagenase I (Invitrogen), 0.1 mg/ml DNase I (Sigma-Aldrich), and 0.015 mg/ml hyaluronidase (Sigma-Aldrich); and cultured in DMEM, 10% FCS, 2 mM L-glutamine, 1 mM sodium pyruvate, 100 U/ml penicillin, 100 µg/ml streptomycin sulfate, and 50 µM 2-mercaptoethanol at 37°C, 8% CO_2. After the fourth passage RA FLSs were grown to confluence and stimulated with PDGF-BB (25 ng/ml; Sigma-Aldrich) for 10 minutes for the signaling studies and 72 hours for the proliferation studies. The RA FLSs used in these studies stained negative with anti-CD68 mAb and exhibited a characteristic fibroblast appearance, suggesting that there were few contaminating macrophages or other cells as described previously (63).

Mast cell stimulation. For IB analysis, C1.MC/57.1 mast cells were serum starved for 6–8 hours, preincubated with imatinib for 2 hours, and stimulated for 10 minutes with SCF (100 ng/ml; PeproTech) and lysates generated. For cytokine analysis, C1.MC/57.1 cells were stimulated with 100 ng/ml SCF for 96 hours and supernatants harvested for cytokine analysis.

Macrophage isolation and stimulation. Resident peritoneal macrophage were isolated from naive DBA/1 mice by i.p. injection and withdrawal of 5–7 ml of complete RPMI media (Invitrogen), and adherent macrophages were cultured overnight in complete DMEM media, pretreated with imatinib for 2 hours, stimulated with M-CSF (100 ng/ml; Chemicon International) for 10 minutes and lysates generated.

B cell isolation and stimulation. B cells were isolated from naive DBA/1 mouse spleens by negative selection with MACS beads (Miltenyi Biotec). Isolated B cells were stimulated for 72 hours with µ-specific anti-IgM F(ab′)₂ (50 µg/ml; MP Biomedicals) or LPS (5 µg/ml; Sigma-Aldrich). For measurement of B cell proliferation, B cells were pulsed with 1 µCi [³H]thymidine (ICN Pharmaceuticals) for the final 18 hours of the stimulation, and a Betaplate scintillation counter (PerkinElmer) was used to quantitate incorporated radioactivity.

T cell stimulation. Splenocytes from anti-CII TCR transgenic mice were stimulated for 72 hours with 0–40 µg/ml whole denatured bovine CII (Chondrex), and [³H]TdR was added for the final 18 hours of culture and radioactivity incorporation quantitated using a Betaplate scintillation counter. For cytokines, cells were stimulated for 72 hours with 20 µg/ml whole denatured bovine CII, and supernatants were harvested for cytokine analysis.

Immunoblotting. Lysates were generated from stimulated peritoneal macrophages, C1.MC/57.1 mast cells, or FLSs (lysis buffer: 1% NP-40, 0.1% SDS, 0.5% sodium deoxycholate, 10 mM EDTA, Halt Protease Inhibitor Cocktail [Pierce Biotechnology], and Phosphatase Inhibitor Cocktail 2 [Sigma-Aldrich]). Lysates were analyzed using standard IB procedures. Briefly, lysates were separated on 7.5% SDS-PAGE gels (Bio-Rad), transferred to PVDF membranes, blocked with milk, and probed with primary and secondary antibodies in BSA, and signal was detected with SuperSignal West Femto Chemiluminescent Substrate (Pierce Biotechnology).

RPP lysate arrays. As previously described (34), lysates were printed on FAST Slides (Whatman) using a robotic microarrayer (Bio-Rad) equipped with solid spotting pins into ordered arrays. Slides were blocked with a 3% casein solution, probed overnight at 4°C overnight with diluted phospho-specific primary antibodies, washed, and probed with HRP-conjugated anti-rabbit IgG antibody (Jackson ImmunoResearch Laboratories Inc.), followed by signal amplification using the Bio-Rad Amplification Reagent (Bio-Rad). Detection of bound biotin was performed with Cy3-streptavidin, and arrays were scanned with a GenePix 4000B scanner (Molecular Devices). Fluorescence intensities were quantified with GenePix 5.0 Pro. Presented values (Figure 3D and Figure 4C) represent anti-protein tyrosine kinase antibody signal (Cy3) normalized to levels in unstimulated cells.

Synovial array analysis. As described previously (37, 38), more than 500 peptides and proteins representing putative autoantigen epitopes were printed on SuperEpoxy slides (TeleChem International Inc.). Each array contained 4–8 duplicate features containing each peptide or protein. Arrays were incubated with 1:150 dilutions of mouse sera, followed by Cy3-labeled anti-mouse IgG/M (Jackson ImmunoResearch Laboratories Inc.), scanned using a GenePix 4000B scanner, and analysis was performed as described (37, 38).

Cytokine analysis. Cytokine analysis was performed using the Beadlyte Human or Mouse Multi-Cytokine Detection System (Chemicon International) and the Luminex 100 System (Luminex Corp.).

Statistics. Visual arthritis scores, paw thicknesses, and histology scores were compared by the Mann-Whitney U test using GraphPad InStat version 3.0 (GraphPad Software). Differences in CIA were determined by Fisher's exact test using the Analyse-it plug-in (Analyse-it) for Excel (Microsoft). Cytokine level comparisons were performed using unpaired 2-tailed Student's t tests (GraphPad Software). SAM (39) and Cluster and TreeView software (64) were used to analyze and display array data. The q value reported by SAM analysis represents the FDR, the likelihood that any individual antigen included in the SAM-determined "hit list" appears on the hit list due to chance (65).

Acknowledgments

Address correspondence to: William H. Robinson, Palo Alto VA Health Care System, 3801 Miranda Avenue, MC 154R, Palo Alto, California 94304, USA. Phone: (650) 849-1207; Fax: (650) 849-1208; E-mail: wrobins@stanford.edu.

1. Firestein, G.S. 2003. Evolving concepts of rheumatoid arthritis. *Nature.* **423**:356–361.
2. Druker, B.J., et al. 2001. Efficacy and safety of a specific inhibitor of the BCR-ABL tyrosine kinase in chronic myeloid leukemia. *N. Engl. J. Med.* **344**:1031–1037.
3. Demetri, G.D., et al. 2002. Efficacy and safety of imatinib mesylate in advanced gastrointestinal stromal tumors. *N. Engl. J. Med.* **347**:472–480.
4. Buchdunger, E., Matter, A., and Druker, B.J. 2001. Bcr-Abl inhibition as a modality of CML therapeutics. *Biochim. Biophys. Acta.* **1551**:M11–M18.
5. Dewar, A.L., et al. 2005. Macrophage colony-stimulating factor receptor c-fms is a novel target of imatinib. *Blood.* **105**:3127–3132.
6. Fabian, M.A., et al. 2005. A small molecule-kinase interaction map for clinical kinase inhibitors. *Nat. Biotechnol.* **23**:329–336.

7. Burmester, G.R., Stuhlmuller, B., Keyszer, G., and Kinne, R.W. 1997. Mononuclear phagocytes and rheumatoid synovitis. Mastermind or workhorse in arthritis? *Arthritis Rheum.* **40**:5–18.

8. Kinne, R.W., Brauer, R., Stuhlmuller, B., Palombo-Kinne, E., and Burmester, G.R. 2000. Macrophages in rheumatoid arthritis. *Arthritis Res.* **2**:189–202.

9. Kontoyiannis, D., Pasparakis, M., Pizarro, T.T., Cominelli, F., and Kollias, G. 1999. Impaired on/off regulation of TNF biosynthesis in mice lacking TNF AU-rich elements: implications for joint and gut-associated immunopathologies. *Immunity.* **10**:387–398.

10. Weinblatt, M.E., et al. 1999. A trial of etanercept, a recombinant tumor necrosis factor receptor:Fc fusion protein, in patients with rheumatoid arthritis receiving methotrexate. *N. Engl. J. Med.* **340**:253–259.

11. Pixley, F.J., and Stanley, E.R. 2004. CSF-1 regulation of the wandering macrophage: complexity in action. *Trends Cell Biol.* **14**:628–638.

12. Wolf, A.M., et al. 2005. The kinase inhibitor imatinib mesylate inhibits TNF-alpha production in vitro and prevents TNF-dependent acute hepatic inflammation. *Proc. Natl. Acad. Sci. U. S. A.* **102**:13622–13627.

13. Woolley, D.E. 2003. The mast cell in inflammatory arthritis. *N. Engl. J. Med.* **348**:1709–1711.

14. Woolley, D.E., and Tetlow, L.C. 2000. Mast cell activation and its relation to proinflammatory cytokine production in the rheumatoid lesion. *Arthritis Res.* **2**:65–74.

15. Benoist, C., and Mathis, D. 2002. Mast cells in autoimmune disease. *Nature.* **420**:875–878.

16. Gordon, J.R., and Galli, S.J. 1990. Mast cells as a source of both preformed and immunologically inducible TNF-alpha/cachectin. *Nature.* **346**:274–276.

17. Nigrovic, P.A., and Lee, D.M. 2005. Mast cells in inflammatory arthritis. *Arthritis Res. Ther.* **7**:1–11.

18. Bromley, M., Fisher, W.D., and Woolley, D.E. 1984. Mast cells at sites of cartilage erosion in the rheumatoid joint. *Ann. Rheum. Dis.* **43**:76–79.

19. Juurikivi, A., et al. 2005. Inhibition of c-kit tyrosine kinase by imatinib mesylate induces apoptosis in mast cells in rheumatoid synovia: a potential approach to the treatment of arthritis. *Ann. Rheum. Dis.* **64**:1126–1131.

20. Lee, D.M., et al. 2002. Mast cells: a cellular link between autoantibodies and inflammatory arthritis. *Science.* **297**:1689–1692.

21. Van den Broek, M.F., van den Berg, W.B., and van de Putte, L.B. 1988. The role of mast cells in antigen induced arthritis in mice. *J. Rheumatol.* **15**:544–551.

22. Cheon, H., et al. 2004. Platelet-derived growth factor-AA increases IL-1beta and IL-8 expression and activates NF-kappaB in rheumatoid fibroblast-like synoviocytes. *Scand. J. Immunol.* **60**:455–462.

23. Watanabe, N., et al. 2002. Gene expression profile analysis of rheumatoid synovial fibroblast cultures revealing the overexpression of genes responsible for tumor-like growth of rheumatoid synovium. *Biochem. Biophys. Res. Commun.* **294**:1121–1129.

24. Remmers, E.F., et al. 1991. Production of platelet derived growth factor B chain (PDGF-B/c-sis) mRNA and immunoreactive PDGF B-like polypeptide by rheumatoid synovium: coexpression with heparin binding acidic fibroblast growth factor-1. *J. Rheumatol.* **18**:7–13.

25. Edwards, J.C., et al. 2004. Efficacy of B-cell-targeted therapy with rituximab in patients with rheumatoid arthritis. *N. Engl. J. Med.* **350**:2572–2581.

26. Nielen, M.M., et al. 2004. Specific autoantibodies precede the symptoms of rheumatoid arthritis: a study of serial measurements in blood donors. *Arthritis Rheum.* **50**:380–386.

27. Kuhn, K.A., et al. 2006. Antibodies against citrullinated proteins enhance tissue injury in experimental autoimmune arthritis. *J. Clin. Invest.* **116**:961–973. doi:10.1172/JCI25422.

28. Miyachi, K., et al. 2003. Efficacy of imatinib mesylate (STI571) treatment for a patient with rheumatoid arthritis developing chronic myelogenous leukemia. *Clin. Rheumatol.* **22**:329–332.

29. Eklund, K.K., and Joensuu, H. 2003. Treatment of rheumatoid arthritis with imatinib mesylate: clinical improvement in three refractory cases. *Ann. Med.* **35**:362–367.

30. Wolff, N.C., Randle, D.E., Egorin, M.J., Minna, J.D., and Ilaria, R.L., Jr. 2004. Imatinib mesylate efficiently achieves therapeutic intratumor concentrations in vivo but has limited activity in a xenograft model of small cell lung cancer. *Clin. Cancer Res.* **10**:3528–3534.

31. Young, J., Liu, C.C., Butler, G., Cohn, Z.A., and Galli, S.J. 1987. Identification, purification, and characterization of a mast cell-associated cytolytic factor related to tumor necrosis factor. *Proc. Natl. Acad. Sci. U. S. A.* **84**:9175–9179.

32. Furuta, G.T., Ackerman, S.J., Lu, L., Williams, R.E., and Wershil, B.K. 1998. Stem cell factor influences mast cell mediator release in response to eosinophil-derived granule major basic protein. *Blood.* **92**:1055–1061.

33. Tsai, M., et al. 1996. The C1.MC/C57.1 (C57) mouse mast cell line is of BALB/c origin and is tumorigenic in BALB/c mice [abstract]. *FASEB J.* **10**:A1253.

34. Chan, S.M., Ermann, J., Su, L., Fathman, C.G., and Utz, P.J. 2004. Protein microarrays for multiplex analysis of signal transduction pathways. *Nat. Med.* **10**:1390–1396.

35. Kakizoe, E., et al. 1999. Increases in mast cells and chymase in fibroproliferative paws of collagen-induced arthritic mice. *Inflamm. Res.* **48**:318–324.

36. Campbell, I.K., Rich, M.J., Bischof, R.J., and Hamilton, J.A. 2000. The colony-stimulating factors and collagen-induced arthritis: exacerbation of disease by M-CSF and G-CSF and requirement for endogenous M-CSF. *J. Leukoc. Biol.* **68**:144–150.

37. Robinson, W.H., et al. 2002. Autoantigen microarrays for multiplex characterization of autoantibody responses. *Nat. Med.* **8**:295–301.

38. Hueber, W., et al. 2005. Antigen microarray profiling of autoantibodies in rheumatoid arthritis. *Arthritis Rheum.* **52**:2645–2655.

39. Tusher, V.G., Tibshirani, R., and Chu, G. 2001. Significance analysis of microarrays applied to the ionizing radiation response. *Proc. Natl. Acad. Sci. U. S. A.* **98**:5116–5121.

40. Osman, G.E., et al. 1998. Expression of a type II collagen-specific TCR transgene accelerates the onset of arthritis in mice. *Int. Immunol.* **10**:1613–1622.

41. Galli, S.J., Nakae, S., and Tsai, M. 2005. Mast cells in the development of adaptive immune responses. *Nat. Immunol.* **6**:135–142.

42. Abdollahi, A., et al. 2005. Inhibition of platelet-derived growth factor signaling attenuates pulmonary fibrosis. *J. Exp. Med.* **201**:925–935.

43. Robinson, W.H., et al. 2003. Protein microarrays guide tolerizing DNA vaccine treatment of autoimmune encephalomyelitis. *Nat. Biotechnol.* **21**:1033–1039.

44. Ho, P.P., et al. 2005. A suppressive oligodeoxynucleotide enhances the efficacy of myelin cocktail/IL-4-tolerizing DNA vaccination and treats autoimmune disease. *J. Immunol.* **175**:6226–6234.

45. Zipfel, P.A., et al. 2000. The c-Abl tyrosine kinase is regulated downstream of the B cell antigen receptor and interacts with CD19. *J. Immunol.* **165**:6872–6879.

46. Genovese, M.C., et al. 2005. Abatacept for rheumatoid arthritis refractory to tumor necrosis factor alpha inhibition. *N. Engl. J. Med.* **353**:1114–1123.

47. Dietz, A.B., et al. 2004. Imatinib mesylate inhibits T-cell proliferation in vitro and delayed-type hypersensitivity in vivo. *Blood.* **104**:1094–1099.

48. Akiyama, T., et al. 1987. Genistein, a specific inhibitor of tyrosine-specific protein kinases. *J. Biol. Chem.* **262**:5592–5595.

49. Akiyama, T., and Ogawara, H. 1991. Use and specificity of genistein as inhibitor of protein-tyrosine kinases. *Methods Enzymol.* **201**:362–370.

50. Satoh, K., et al. 2001. Involvement of ErbB-2 in rheumatoid synovial cell growth. *Arthritis Rheum.* **44**:260–265.

51. Kehlen, A., Thiele, K., Riemann, D., and Langner, J. 2002. Expression, modulation and signalling of IL-17 receptor in fibroblast-like synoviocytes of patients with rheumatoid arthritis. *Clin. Exp. Immunol.* **127**:539–546.

52. Verdrengh, M., Jonsson, I.M., Holmdahl, R., and Tarkowski, A. 2003. Genistein as an anti-inflammatory agent. *Inflamm. Res.* **52**:341–346.

53. Druker, B.J. 2002. Inhibition of the Bcr-Abl tyrosine kinase as a therapeutic strategy for CML. *Oncogene.* **21**:8541–8546.

54. Ando, W., et al. 2006. Imatinib mesylate inhibits osteoclastogenesis and joint destruction in rats with collagen-induced arthritis (CIA). *J. Bone Miner. Metab.* **24**:274–282.

55. Miyagawa, S., Fujimoto, H., Ko, S., Hirota, S., and Kitamura, Y. 2002. Improvement of psoriasis during imatinib therapy in a patient with a metastatic gastrointestinal stromal tumour. *Br. J. Dermatol.* **147**:406–407.

56. Sadanaga, A., et al. 2005. Amelioration of autoimmune nephritis by imatinib in MRL/lpr mice. *Arthritis Rheum.* **52**:3987–3996.

57. Davidson, A., and Diamond, B. 2001. Autoimmune diseases. *N. Engl. J. Med.* **345**:340–350.

58. Camps, M., et al. 2005. Blockade of PI3Kgamma suppresses joint inflammation and damage in mouse models of rheumatoid arthritis. *Nat. Med.* **11**:936–943.

59. Nagar, B., et al. 2002. Crystal structures of the kinase domain of c-Abl in complex with the small molecule inhibitors PD173955 and imatinib (STI-571). *Cancer Res.* **62**:4236–4243.

60. Arnett, F.C., et al. 1988. The American Rheumatism Association 1987 revised criteria for the classification of rheumatoid arthritis. *Arthritis Rheum.* **31**:315–324.

61. Coligan, J.E., Kruisbeek, A.M., Margulies, D.H., Shevach, E.M., and Strober, W. 1994. Collagen-induced arthritis. In *Current protocols in immunology* [book on CD-ROM]. John Wiley and Sons Inc. Hoboken, New Jersey, USA. 15.15.11–15.15.24.

62. Deng, G.M., Zheng, L., Chan, F.K., and Lenardo, M. 2005. Amelioration of inflammatory arthritis by targeting the pre-ligand assembly domain of tumor necrosis factor receptors. *Nat. Med.* **11**:1066–1072.

63. Valencia, X., et al. 2004. Cadherin-11 provides specific cellular adhesion between fibroblast-like synoviocytes. *J. Exp. Med.* **200**:1673–1679.

64. Eisen, M.B., Spellman, P.T., Brown, P.O., and Botstein, D. 1998. Cluster analysis and display of genome-wide expression patterns. *Proc. Natl. Acad. Sci. U. S. A.* **95**:14863–14868.

65. Storey, J.D. 2002. A direct approach to false discovery rates. *J. R. Stat. Soc.* **64**:479–498.